New Implementation of Nearest Vector Selecting Space Vector Control for Three-Phase Multilevel Voltage Source Inverter

Lopatkin N.N.
Mathematics, Physics and Informatics Department
Shukshin Altai State Humanities Pedagogical University (ASHPU)
Biysk, Russia
nikolay_lopatkin@mail.ru

***Abstract*—The paper offers a more simple alternative to the well known space vector control algorithm with the nearest vector selection for three-phase multilevel voltage source inverters with enough high number of levels. This space vector control is righteously considered to be one of the most promising algorithms for medium and high voltage converters providing sufficient voltage quality at low switching frequency. The offered technique has been developed in the context of the space vector algorithm of two delta voltages which use barycentric and affine (oblique-angled) coordinates on triangles of three nearest vectors to the reference one. This approach to space vector control for an arbitrary number of inverter levels needs no preliminary finding of any coefficients and holding them in look-up tables.**

Keywords—multilevel inverter; voltage space vector control (SVC); barycentric coordinates; oblique-angled coordinates; integer and fractional parts of delta voltages relative values; quarter-wave symmetry

I. INTRODUCTION

The multilevel voltage source inverters (MLVSI) have became mainstream converters with AC output voltage. Now they are really ready for application in industry, including both adjustable frequency induction motor drive and AC voltage generation by the renewable energy sources [1]-[7].

The same inverter power circuit might be controlled by different ways leading to different output, input and itself inverter related performances. So, the modulation technique becomes the main instrument to provide high quality output AC voltage and current, high output capability, low losses in power switches, low cost of components or anything else parameters or acceptable combinations of the parameters values [8]-[12].

With a growing number of the MLVSI levels carrier-based modulation techniques become less and less attractive due to the growing number of the carriers and stricter requirements to their parameters values. So, the space vector modulation should be brought to the forefront while medium and high voltage converters control technique is being chosen. In particular, the so-called space vector control (SVC) righteously considered to be one of the most promising algorithms for industrial medium and high voltage converters with enough high number of levels, provides both high voltage quality and low transistors switching frequency of cascaded multilevel inverter (CMLI) [13]-[16]. The further development of this technique has been its variant for the CMLI common-mode voltage reduction due to selection of the vectors with the zero common-mode voltage [17].

II. PROBLEM DEFINITION

The conventional basic SVC algorithm [13]-[16] for any sampling cycle replaces nearest three vectors switching sequence with the action of the only space vector which is the nearest to the reference voltage space vector (RVSV) at the sampling moment.

This SVC technique uses the RVSV vector presented in normalized orthogonal components:

$$u^{\circ}_{REF} = u^{\circ}_{REFx} + j \cdot u^{\circ}_{REFy}, \tag{1}$$

$$u^{\circ}_{REFx} = \frac{u_{REFx}}{U_d/3} = 2 \cdot u^{*}_{REFaN} - u^{*}_{REFbN} - u^{*}_{REFcN}, \tag{2}$$

$$u^{\circ}_{REFy} = \frac{u_{REFy}}{U_d/\sqrt{3}} = u^{*}_{REFbN} - u^{*}_{REFcN}, \tag{3}$$

where u^{*}_{w} is the relative voltage value for arbitrary voltage u_w, $u^{*}_{w} = u_w / U_d$, U_d is the input DC voltage of the unit (base) level.

According to the technique, the current position of the RVSV on voltage vectors diagram relates to the rectangle whose vertex (that is the farthest from the origin) has coordinates

$$n_x = \mathrm{sgn}\left(u^{\circ}_{REFx}\right) \cdot \left\lceil \left| u^{\circ}_{REFx} \right| \right\rceil, \; n_y = \mathrm{sgn}\left(u^{\circ}_{REFy}\right) \cdot \left\lceil \left| u^{\circ}_{REFy} \right| \right\rceil, \tag{4}$$

where $\lceil w \rceil$ means the rounding up w to the closest integer number (the "ceiling" function), $\mathrm{sgn}(w)$ is the standard sign function.

Whole the vector diagram complex plane should be preliminary marked with rectangles corresponding to the integer values of coordinates x° and y° which are x and y

978-1-5386-4307-5/18/$31.00 ©2018 IEEE

normalized similar to (2) and (3). As soon as the RVSV position rectangle k is identified, u°_{REFy} is being compared with value of expression $y^{\circ}_{k}\left(u^{\circ}_{REFy}\right)=a_k\cdot u^{\circ}_{REFy}+b_k$ in order to choose one of the two inverter vectors belonging to different hexagons of the highest proximity locus and to assign it to executed voltage space vector (EVSV). So, the a_i and b_i values should be preliminary assigned for every of the rectangles and held in look-up tables.

Resorting to consideration of (2) and (3) expressions, one can notice that normalized orthogonal components are related to relative delta voltages:

$$u^{\circ}_{REFx}=u^{*}_{REFab}-u^{*}_{REFca},\ u^{\circ}_{REFy}=u^{*}_{REFbc}. \tag{5}$$

It seems reasonable to operate with the set of reference delta voltages in a more explicit way and to apply to them some different rounding function instead of used in (4). Fortunately, the appropriate approach has been already designed for the three vectors processing which are the nearest to the RVSV vector.

As a further development of research in [18] and [19] in the area of space vector modulation (SVM) for MLVSI, dealing with the oblique-angled coordinates of two delta voltages for simplification of the basic calculations in MLVSI space voltage PWM (SVPWM) algorithms, new investigations were accomplished resulting in some interesting findings [20]-[28]. In particular, [20] shows the occurrence and the kinds of the oblique-angled coordinates, [21] describes the possible barycentric and affine space vector coordinates on triangles, underlines the role of the integer and fractional parts of the delta voltages relative values as the coordinates and the duty cycles of the three nearest vectors, and offers the several two-coordinate and three-coordinate effective algorithms for finding the coordinates and the duty cycles of the being executed vectors. A new symmetric and easy calculated triangle type identifier is presented in [21], [22]. At last, the enough fast resource saving algorithm implementations on the base of the nonconventional five-segment and three-segment switching sequence schemes are offered in [22]-[28] where their output voltage quality harmonic indices are presented.

The vectors of a four-level MLVSI variant in the context of the used $\left(u^{*}_{ab},u^{*}_{bc}\right)$ oblique-angled coordinates are shown in Fig. 1.

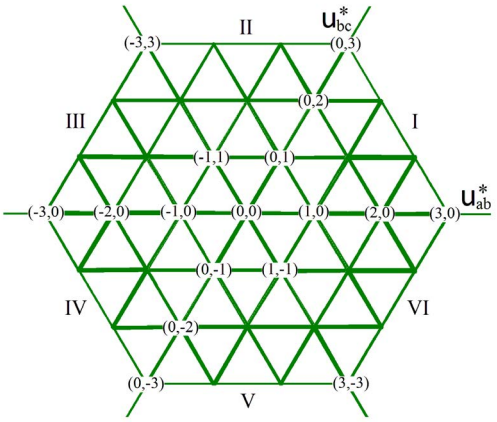

Fig. 1. Voltage vectors diagram in oblique-angled 60-degree coordinates.

The purpose of this paper is to demonstrate opportunities of processing just the integer and fractional parts of the relative delta voltages values for implementation the same resulting EVSV as is provided by SVC technique proposed in [13]-[16].

III. New Nearest Vector Selecting Technique

The offered here scheme applies no special operations radically different from used in the traditional one. But it utilizes the conventional SVPWM attribute, namely "modulating triangle" of the three vectors nearest to the reference voltage space vector RVSV (NTV).

Fig. 2. shows a vector diagram fragment containing the RVSV vector endpoint R, namely the rhombus of the four vectors nearest to the point R, under the following condition for every of the three delta voltages relative values:

$$u^{*}_{gh}\neq\left\lfloor u^{*}_{gh}\right\rfloor. \tag{6}$$

Here $\lfloor w\rfloor$ is the integer part of w, i.e. the rounding down w to the closest integer number, taking into account the sign (the "floor" function), $\{w\}$ means the fractional part of w, $\{w\}=w-\lfloor w\rfloor$.

The space vectors can be represented both as 3-dimensional $\left(u^{*}_{ab},u^{*}_{bc},u^{*}_{ca}\right)$ and 2-dimensional $\left(u^{*}_{ab},u^{*}_{bc}\right)$ vectors, as well as $\left(u^{*}_{ba},u^{*}_{cb},u^{*}_{ac}\right)$ and $\left(u^{*}_{ba},u^{*}_{cb}\right)$ vectors through the introduction of the three opposite sign relative delta voltages:

$$u^{*}_{REFhg}=-u^{*}_{REFgh}. \tag{7}$$

The rhombus vertices in Fig. 2. are defined in $\left(u^{*}_{ab},u^{*}_{bc}\right)$ and $\left(u^{*}_{ba},u^{*}_{cb}\right)$ coordinates via a current position the RVSV vector. As can be seen, provided (6) is fulfilled, the following equations are valid:

$$\left\lfloor u^{*}_{REFab}\right\rfloor=-1-\left\lfloor u^{*}_{REFba}\right\rfloor,\ \left\lfloor u^{*}_{REFbc}\right\rfloor=-1-\left\lfloor u^{*}_{REFcb}\right\rfloor, \tag{8}$$

$$\left\{u^{*}_{REFab}\right\}=1-\left\{u^{*}_{REFba}\right\},\ \left\{u^{*}_{REFbc}\right\}=1-\left\{u^{*}_{REFcb}\right\}. \tag{9}$$

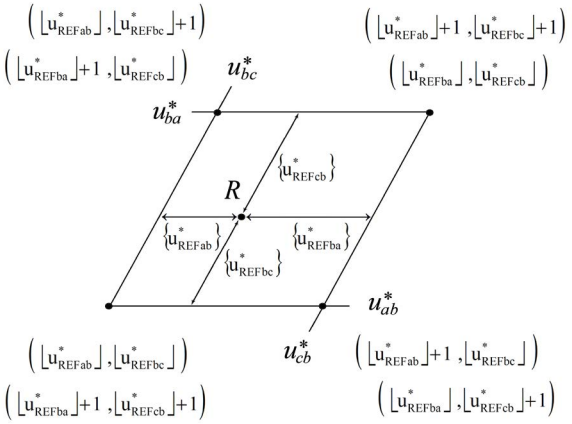

Fig. 2. Integer and fractional parts of reference delta voltages relative values as coordinates of the four nearest vectors, and reference vector position identifiers, respectively.

It should be noted that in case of one or all of the three relative delta voltages values turn out to be integer (condition (6) is not respected), the RVSV endpoint hits exactly to the line or to the vertex of the rhombus, respectively. In these cases, the second system coordinates of the rhombus vertices in Fig. 2 become wrong.

As have been shown in [21], the fractional parts of the reference delta voltages relative values are not only the duty cycles of the three nearest vectors NTV in SVPWM, but also the barycentric coordinates on corresponding triangle for the reference voltage space vector RVSV endpoint. So, the closer to unity the fractional value of certain relative delta voltage is, the closer to the related vertex the RVSV endpoint is. Moreover, the highest value of the three barycentric coordinates on the NTV triangle makes it possible to recognize the appropriate vertex as the closest to the reference point, and such a way one can choose the space vector nearest to the vector RVSV endpoint.

Fig. 3 demonstrates duty cycles values of the three vectors nearest to the sampled RVSV over the SVPWM clock cycle (the RVSV endpoint barycentric coordinates) for both up-pointing and down-pointing triangle types [21].

Due to the fractional parts of the reference delta voltages relative values are mapped to the possible nearest vectors, the closest to the reference RVSV voltage space vector is being found easily through the comparisons of the three fractional values for maximum value detection in one of the two triangles.

In accordance with the concept of operating with the only two independent delta voltages, both reference RVSV and executed EVSV voltage space vectors are treated as two-coordinate vectors in $\left(u^*_{ab}, u^*_{bc}\right)$ plane.

The main used in [22-28] the delta voltage two-component formation principle is kept in the offered here approach:

$$u^*_{EXEgh}(t) = \left\lfloor u^*_{REFgh}(t) \right\rfloor + f_{EXEgh}(t), \tag{10}$$

where the relative value of the being executed output delta voltage $u^*_{EXEgh}(t)$ and its two components are instantaneous functions of current time, the relative value of the reference delta voltage $u^*_{REFgh}(t)$ is here assumed to be continuous function, $\left\lfloor u^*_{REFgh}(t) \right\rfloor$ is stepped function, and $f_{EXEgh}(t)$ is the pulse function that can possess only the values 0 and 1. It may be called a "fractional component function", since it is determined by comparing of the only fractional parts of the reference delta voltages relative values.

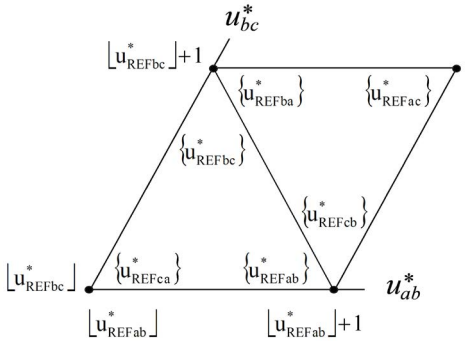

Fig. 3. Integer and fractional parts of reference delta voltages relative values as coordinates and duty cycles of the three nearest vectors over the SVPWM clock cycle.

In order to write mathematical expressions in compact form, let's introduce designations

$$b_{gh}(t) = \left\{u^*_{REFgh}(t)\right\},\ b_{hg}(t) = \left\{u^*_{REFhg}(t)\right\}, \tag{11}$$

e.g. $b_{ab}(t) = \left\{u^*_{REFab}(t)\right\},\ b_{ba}(t) = \left\{u^*_{REFba}(t)\right\}$ etc.

These quantities becomes the reference vector RVSV barycentric coordinates $\left(b_{ab\Delta}, b_{bc\Delta}, b_{ca\Delta}\right)$ on the NTV up-pointing triangle (related to voltages $u^*_{REFgh}(t)$ considered in coordinate system $\left(u^*_{ab}, u^*_{bc}, u^*_{ca}\right)$) and $\left(b_{ba\Delta}, b_{cb\Delta}, b_{ac\Delta}\right)$ on the NTV down-pointing triangle (related to voltages $u^*_{REFhg}(t)$ considered in coordinate system $\left(u^*_{ba}, u^*_{cb}, u^*_{ac}\right)$) while the RVSV endpoint stays in the corresponding NTV triangle: $b_{gh\Delta}(t) = b_{gh}(t)$, $b_{hg\Delta}(t) = b_{hg}(t)$, e.g. $b_{ab\Delta}(t) = b_{ab}(t)$, $b_{ba\Delta}(t) = b_{ba}(t)$ etc.

Certainly, for the two NTV triangle types

$$b_{ab\Delta}(t) + b_{bc\Delta}(t) + b_{ca\Delta}(t) = 1,$$
$$b_{ba\Delta}(t) + b_{cb\Delta}(t) + b_{ac\Delta}(t) = 1. \tag{12}$$

For the case of the up-pointing NTV triangle type, the new nearest vector selecting technique uses the simple rule of the second component of (10) finding, based on Fig. 3 consideration:

$$f_{EXEgh}(t) = \begin{cases} 1, & \text{if } b_{gh\Delta}(t) = \max\left(b_{ab\Delta}(t), b_{bc\Delta}(t), b_{ca\Delta}(t)\right); \\ 0, & \text{otherwise.} \end{cases} \tag{13}$$

According to Fig. 2 and (8), the same rule is applied to the down-pointing NTV triangle type:

$$f_{EXEhg}(t) = \begin{cases} 1, & \text{if } b_{hg\Delta}(t) = \max\left(b_{ba\Delta}(t), b_{cb\Delta}(t), b_{ac\Delta}(t)\right); \\ 0, & \text{otherwise.} \end{cases} \tag{14}$$

Rules (13) and (14) let (10) be valid for every of all six delta voltages of the both coordinate systems $\left(u^*_{ab}, u^*_{bc}, u^*_{ca}\right)$ and $\left(u^*_{ba}, u^*_{cb}, u^*_{ac}\right)$, but they can be reduced to following two propositional functions defining the components of the two base executed voltages of $\left(u^*_{ab}, u^*_{bc}\right)$ plane for any NTV triangle type, taking into account (12) and (9):

$$f_{EXEab}(t) = \left(F_\Delta(t) \cap f_{ab1}(t) \cap f_{ab2}(t)\right) \cup \left(F_\nabla(t) \cap \left(f_{ab1}(t) \cup f_{ab2}(t)\right)\right), \tag{15}$$

$$f_{EXEbc}(t) = \left(F_\Delta(t) \cap f_{bc1}(t) \cap f_{bc2}(t)\right) \cup \left(F_\nabla(t) \cap \left(f_{bc1}(t) \cup f_{bc2}(t)\right)\right), \tag{16}$$

where $F_\Delta(t)$, $F_\nabla(t)$, $f_{ab1}(t)$, $f_{ab2}(t)$, $f_{bc1}(t)$ and $f_{bc2}(t)$ are propositional expressions that can possess only the values

0 and 1, $F_{\Delta}(t)$ and $F_{\nabla}(t)$ are respectively the up-pointing and down-pointing NTV triangle type identifiers [21], [22]. All these variables are defined as follows:

$$F_{\Delta}(t)=\lfloor u^{*}_{REFab}\rfloor+\lfloor u^{*}_{REFbc}\rfloor+\lfloor u^{*}_{REFca}\rfloor+2\,,\ F_{\nabla}(t)=\overline{F}_{\Delta}(t)\,,$$
$$f_{ab1}(t)\equiv b_{ab}(t)>b_{bc}(t)\,,\ f_{ab2}(t)\equiv b_{ab}(t)>b_{ca}(t)\,,$$
$$f_{bc1}(t)\equiv b_{bc}(t)>b_{ca}(t)\,,\ f_{bc2}(t)\equiv b_{bc}(t)>b_{ab}(t)\equiv \bar{f}_{ab1}(t)\,,$$
$$b_{ca\Delta}(t)=1-b_{ab\Delta}(t)-b_{bc\Delta}(t)=1-b_{ab}(t)-b_{bc}(t)\,, \quad (17)$$

here $\overline{w}$ is the logical inversion of w; unlike $b_{ab\Delta}(t)$ and $b_{bc\Delta}(t)$, $b_{ca\Delta}(t)$ might be not equal to $b_{ca}(t)$, namely $b_{ca\Delta}(t)=b_{ca}(t)$ for the up-pointing NTV triangle type and $b_{ca\Delta}(t)=b_{ca}(t)-1$ for the down-pointing NTV triangle type.

So, (10) and (15)-(17) establish the scheme for the nearest vector selecting space vector control for any three-phase multilevel voltage source inverter with arbitrary number of the regular levels via determining the executed EVSV voltage space vector $\left(u^{*}_{EXEab},u^{*}_{EXEbc}\right)$ instantaneous values:

$$\begin{bmatrix} u^{*}_{EXEab}(t)\\ u^{*}_{EXEbc}(t)\end{bmatrix}=\begin{bmatrix} \lfloor u^{*}_{REFab}(t)\rfloor+f_{EXEab}(t)\\ \lfloor u^{*}_{REFbc}(t)\rfloor+f_{EXEbc}(t)\end{bmatrix}. \quad (18)$$

The resulting phase-to-neutral executed voltages can be described by the well known matrix equation:

$$\begin{bmatrix} u^{*}_{EXEan}(t)\\ u^{*}_{EXEbn}(t)\\ u^{*}_{EXEcn}(t)\end{bmatrix}=\frac{1}{3}\cdot\begin{bmatrix} 2 & 1\\ -1 & 1\\ -1 & -2\end{bmatrix}\cdot\begin{bmatrix} u^{*}_{EXEab}(t)\\ u^{*}_{EXEbc}(t)\end{bmatrix}, \quad (19)$$

Hereinafter subscript g will denote the "ground", i.e. the MLVSI feeding voltage zero node.

The directly executed phase-to-ground voltages can be chosen in accordance with the following description [18], [20]:

$$\begin{bmatrix} u^{*}_{EXEag}(t)\\ u^{*}_{EXEbg}(t)\\ u^{*}_{EXEcg}(t)\end{bmatrix}=\begin{bmatrix} k(t)\\ k(t)-u^{*}_{EXEab}(t)\\ k(t)-u^{*}_{EXEab}(t)-u^{*}_{EXEbc}(t)\end{bmatrix}, \quad (20)$$

where $k(t)$ can possess the only integer values,

$$k_{\min}(t)\le k(t)\le k_{\max}(t)\,,$$
$$k_{\min}(t)=\max\left(0,u^{*}_{EXEab}(t),u^{*}_{EXEab}(t)+u^{*}_{EXEbc}(t)\right), \quad (21)$$
$$k_{\max}(t)=\min\left(N,N+u^{*}_{EXEab}(t),N+u^{*}_{EXEab}(t)+u^{*}_{EXEbc}(t)\right),$$

N is the number of MLVSI levels, i.e. the number of different voltage values provided by one MLVSI phase leg.

Changing $u^{*}_{EXEag}(t)$ between tracks from $k_{\min}(t)$ to $k_{\max}(t)$ (while the track is not the only one) can be used for leveling of the voltages across the capacitors applied in the basic types of the MLVSI.

The obtained controller functions of the executed phase-to-ground voltages (20) make it possible to generate gating pulses for phase legs semiconductor switches in different MLVSI topologies.

IV. Simulation Results

The appropriate to equations (18), (20) and (21) controller, being the core part of Matlab/Simulink model, is presented in Fig.4 for $k(t)=k_{\min}(t)$, i.e. for the case of the minimum instantaneous phase-to-ground voltages values.

The Matlab/Simulink-simulated idealized (controller) waveforms of the output delta voltage u^{*}_{EXEbc}, the phase-to-neutral voltage u^{*}_{EXEbn} and the phase-to-ground voltage u^{*}_{EXEbg}, as well as the PSIM-simulated delta voltage spectrum are presented for the delta voltage amplitude modulation index $m_{a\Delta}$ values 3.5 and 12.6 in Fig. 5 and Fig. 6, respectively.

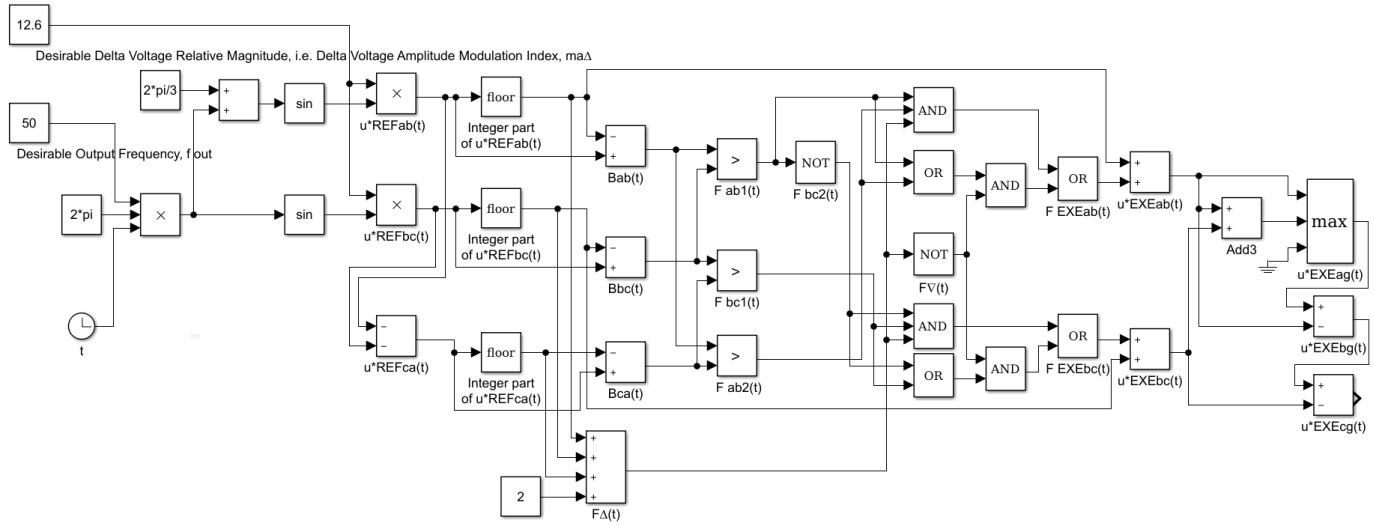

Fig. 4. New nearest vector selecting space vector controller for three-phase multilevel voltage source inverter with arbitrary level number N.

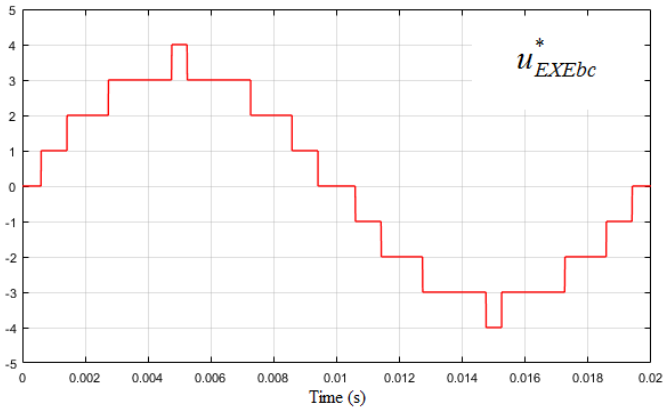

a)

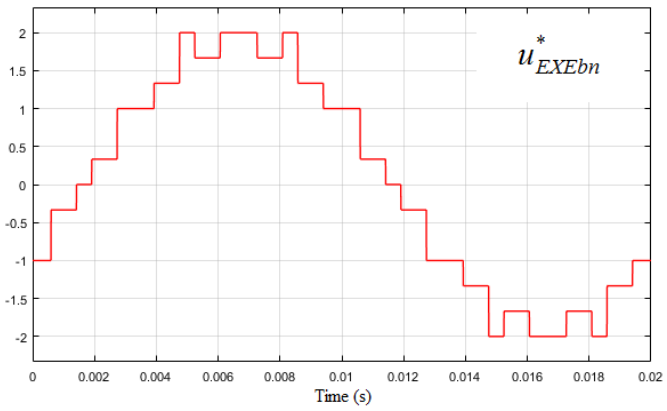

b)

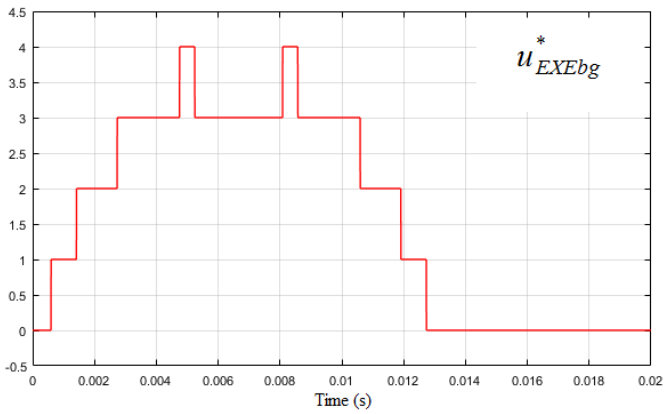

c)

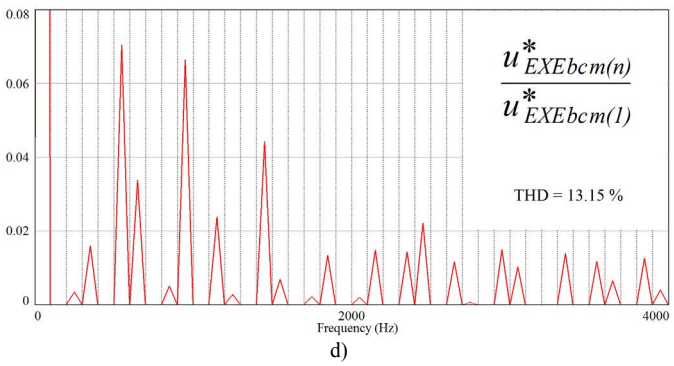

d)

Fig. 5. Simulated results for $m_{a\Delta}$ = 3.5: Simulink waveforms of output delta voltage a), phase-to-neutral voltage b), and phase-to-ground voltage c); PSIM delta voltage spectrum d).

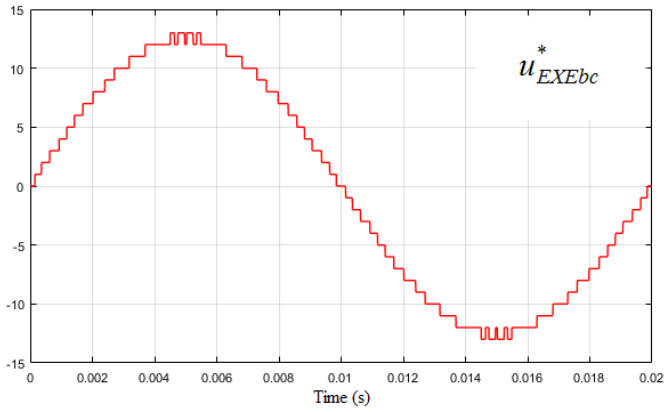

a)

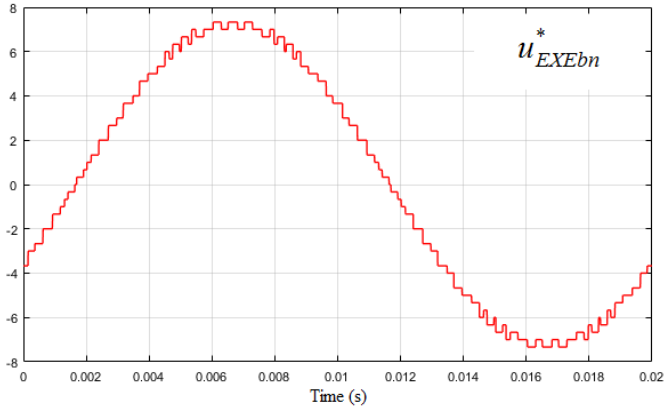

b)

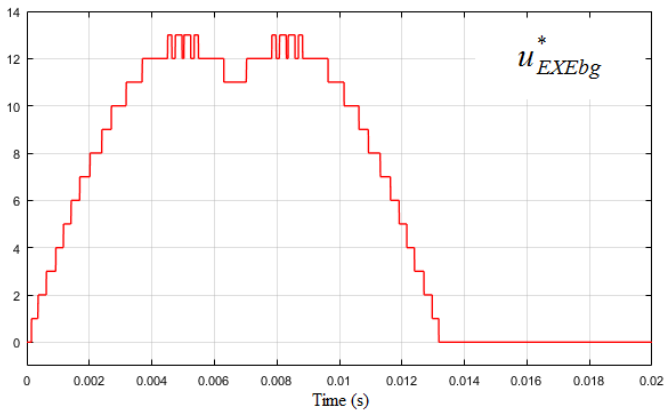

c)

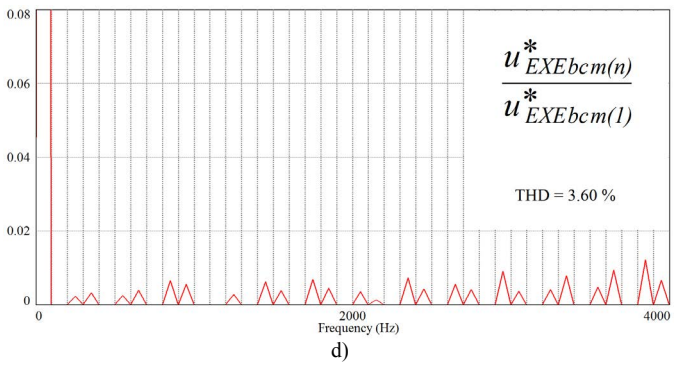

d)

Fig. 6. Simulated results for $m_{a\Delta}$ = 12.6: Simulink waveforms of output delta voltage a), phase-to-neutral voltage b), and phase-to-ground voltage c); PSIM delta voltage spectrum d).

The used here delta voltage amplitude modulation index is defined as follows:

$$m_{a\Delta} = \sqrt{3} \cdot U / U_d = \sqrt{3} \cdot U^* = U^*_{\Delta m}, \quad (22)$$

where U and U^* are the value and the relative value of the reference voltage space vector magnitude, respectively, $U^*_{\Delta m}$ is the amplitude relative value of the reference delta voltages.

The resulting delta and phase-to-neutral voltage waveforms have the quarter-wave symmetry and contain the same orders harmonics at any values of the amplitude modulation index, namely harmonics with numbers $n = 6 \cdot k \pm 1$, where k belongs to the natural numbers.

Such the analog control might be treated as digital one with the tending to zero sampling period duration, and this case shows the boundaries of voltage quality for this kind of SVC upon non-zero sampling period, in particular THD exact theoretical lower limit.

V. Conclusions

The new implementation of the space vector control algorithm with the nearest vector selection for three-phase multilevel voltage source inverters is presented.

The offered technique uses both the integer part and the fractional part of the reference delta voltages relative values as the coordinates of the reference voltage space vector. This approach to space vector control for any arbitrary circuit of the voltage source multilevel inverter with any arbitrary number of the equal feeding DC voltage levels needs no preliminary finding of anything coefficients and holding them in look-up tables.

The thorough research is needed to estimate not only the THD but also the integral factors of harmonics (including the weighted THD) of the resulting MLVSI voltage as functions of the amplitude modulation index. These factors make it possible to evaluate beforehand the load current quality, in particular its THD value.

The demonstrated here model and the results are mostly related to the analog control scheme, so supplementary investigation is necessary to assess the impact of the reference voltages sample rate on the output voltages quality.

The space vector control should be treated as the most promising technique for industrial application due to the output voltage has enough high quality at low switching frequency, provided that DC voltage levels are accessible in sufficient numbers.

References

[1] Bin Wu and M. Narimani, High-Power Converters and AC Drives. Wiley-IEEE Press, 2017.

[2] S. Kouro, M. Malinowski, K. Gopakumar, J. Pou, L.G. Franquelo, Bin Wu, J. Rodriguez, M.A. Pérez, and J.I. Leon, "Recent advances and industrial applications of multilevel converters," IEEE Transactions on Industrial Electronics, vol. 57, is. 8, pp. 2553-2580, 2012.

[3] S.A. Gonzalez, S.A. Verne, and M.I. Valla, Multilevel Converters for Industrial Applications. CRC Press, 2013.

[4] F.L. Luo and H. Ye, Advanced DC/AC Inverters: Applications in Renewable Energy. CRC Press, 2013.

[5] B. Ge, F.Z. Peng, and Y. Li, "Multilevel Converter/Inverter Topologies and Applications," Chapter 14 in Power Electronics for Renewable Energy Systems, Transportation and Industrial Applications, pp. 422-462, 2014.

[6] S. Stynski and M. Malinowski, "Space Vector Modulation in Three-Phase Three-Level Flying Capacitor Converter-Fed Adjustable Speed Drive," Chapter 10 in Advanced and Intelligent Control in Power Electronics and Drives, pp. 335-374, 2014.

[7] E.C. dos Santos and E.R.C. da Silva, Advanced Power Electronics Converters: PWM Converters Processing AC Voltages. Wiley-IEEE Press, 2015.

[8] J. Rodriguez, J.-S. Lai, and F.Z. Peng, "Multilevel inverters: a survey of topologies, controls, and applications," IEEE Transactions on Industrial Electronics, vol. 49, is. 4, pp. 724-738, 2002.

[9] D.G. Holms and T.A. Lipo, Pulse Width Modulation for Power Converters. Piscataway. NJ: IEEE Press, 2003.

[10] J.I. Leon, S. Kouro, J. Rodriguez, and Bin Wu, "The essential role and the continuous evolution of modulation techniques for voltage-source inverters in the past, present, and future power electronics," IEEE Transactions on Industrial Electronics, vol. 63, is. 5, pp. 2688-2701, 2016.

[11] I.A. Bakhovtsev and G.S. Zinoviev, "Generalized analysis of output power of multiphase multilevel PWM voltage source inverters," Electricity, is. 4, pp. 26-33, 2016.

[12] I.A. Bakhovtsev and G.S. Zinovev, "PWM methods evolution," APEIE-2016, 13th Int. Conf. on Actual Problems of Electronic Instrument Engineering, vol. 10, pp. 129-144, 2016.

[13] J. Rodriguez, L. Moran, C. Silva, and P. Correa, "A high performance vector control of a 11-level inverter," IPEMC 2000, 3rd Int. Power Electronics and Motion Control Conf., pp. 1116-1121, 2000.

[14] J. Rodriguez, P. Correa, and L. Moran, "A vector control technique for medium voltage multilevel inverters," APEC 2001, 16th Annual IEEE Applied Power Electronics Conf. and Exposition, pp. 173-178, 2001.

[15] J. Rodriguez, L. Moran, P. Correa, and C. Silva, "A vector control technique for medium-voltage multilevel inverters," IEEE Transactions on Industrial Electronics, vol. 49, is. 4, pp. 882-888, 2002.

[16] J. Rodriguez, L. Moran, J. Pontt, P. Correa, and C. Silva, "A high-performance vector control of an 11-level inverter," IEEE Transactions on Industrial Electronics, vol. 50, is. 1, pp. 80-85, 2003.

[17] J. Rodriguez, J. Pontt, P. Correa, P. Cortes, and C. Silva, "A new modulation method to reduce common-mode voltages in multilevel inverters," IEEE Transactions on Industrial Electronics, vol. 51, is. 4, pp. 834-839, 2004.

[18] N. Celanovic and D. Boroyevich, "A fast space-vector modulation algorithm for multilevel three-phase converters," IEEE Transactions on Industry Applications, vol. 37, is. 2, pp. 637-641, 2001.

[19] L.G. Castro, M.B. Correa, C.B. Jacobina, and D. Boroyevich, "A fast space-vector algorithm for multilevel converters without coordinates transformation," 2010 IEEE Energy Conversion Congress and Exposition (ECCE), pp. 2543-2547, 2010.

[20] N.N. Lopatkin, "Representation of the voltage space vector of the multilevel inverter in oblique-angled coordinate systems of two delta voltages," APEIE-2014, 12th Int. Conf. on Actual Problems of Electronic Instrument Engineering, vol. 1, pp. 824-828, 2014.

[21] N.N. Lopatkin, "Some new representations of the multilevel inverter voltage space vector in the complex plane," SIBCON-2015, 2015 Int. Siberian Conf. on Control and Communications (SIBCON), no. CFP15794-CDR, 2015.

[22] N.N. Lopatkin, "Simple delta voltages space vector PWM algorithm for voltage source multilevel inverters," 2016 2-nd Int. Conf. on Intelligent Energy and Power Systems (IEPS), no. CFP1605X-PRT, pp. 149-154, 2016.

[23] N.N. Lopatkin, "Output voltage simulation of multilevel inverter with space vector modulation of two delta voltages," Technical Electrodynamics, is. 5, pp. 20-22, 2016.

[24] N.N. Lopatkin, "Voltage harmonics integral factors estimation of multilevel inverter with space vector modulation of two delta voltages," APEIE-2016, 13th Int. Conf. on Actual Problems of Electronic Instrument Engineering, vol. 1, part 3, pp. 112-115, 2016.

[25] N.N. Lopatkin, "Voltage quality comparison of space vector PWM voltage source multilevel inverter under symmetric and nonsymmetric switching sequence variants: voltage waveforms, spectra and THD,"

ICIEAM-2017, 2017 3rd Int. Conf. on Industrial Engineering, Applications and Manufacturing (ICIEAM), no. 40534, pp. 1-8, 2017.

[26] N.N. Lopatkin and G.S. Zinoviev, "Voltage quality comparison of space vector PWM voltage source multilevel inverter under symmetric and nonsymmetric switching sequence variants: voltage harmonics integral factors," ICIEAM-2017, 2017 3rd Int. Conf. on Industrial Engineering, Applications and Manufacturing (ICIEAM), no. 40534, pp. 1-7, 2017.

[27] N.N. Lopatkin, "Simple space vector PWM scheme with quarter-wave symmetric output voltage waveform for three-phase multilevel inverter," 2017 Int. Multi-Conf. on Engineering, Computer and Information Sciences (SIBIRCON), pp. 433-438, 2017.

[28] N.N. Lopatkin, "Voltage source multilevel inverter voltage quality comparison under multicarrier sinusoidal PWM and space vector PWM of two delta voltages," 2017 Int. Multi-Conf. on Engineering, Computer and Information Sciences (SIBIRCON), pp. 439-444, 2017.